ANALYTICAL SCIENCES AUGUST 2018, VOL. 34

Damage-less Handling of Exosomes Using an Ion-depletion Zone in a Microchannel

Katsuo MOGI,*,† Kei HAYASHIDA,*** and Takatoki YAMAMOTO***†**

**Functional Proteomics Team, Molecular Profiling Research Center for Drug Discovery, National Institute of Advanced Industrial Science and Technology, 2-4-7 Aomi, Koto, Tokyo 135–0064, Japan*
***Department of Biological Science, Graduate School of Bioscience and Biotechnology, Tokyo Institute of Technology, 2-12-1 Ookayama, Meguro, Tokyo 152–8552, Japan*
****Department of Mechanical Engineering, Tokyo Institute of Technology, 2-12-1 Ookayama, Meguro, Tokyo 152–8552, Japan*

Exosomes are of increasing research interest because they are integral to cell–cell communication and are implicated in various disease states. Here, we investigated the utility of using an ion-depletion zone in a microfluidic device to concentrate exosomes from the culture media of four types of cell lines. Furthermore, we evaluated the extent of damage to the exosomes following concentration by an ion-depletion zone microchannel device compared with exosomes concentrated by a conventional ultra-centrifugation technique. Our results conclusively demonstrate that significantly less damage is incurred by exosomes following passage through and concentration by the ion-depleted zone microchannel device compared to concentration by ultra-centrifugation. Our findings will help extend the utility of exosomes to various applications.

Keywords Exosome, ion-exchange membrane, ion-depletion zone, ion-concentration polarization, concentration

(Received September 8, 2017; Accepted March 5, 2018; Published August 10, 2018)

Introduction

Cells in multicellular organisms communicate with each other to maintain the health of the organism. This communication can sometimes facilitate the progression of disease.[1] Exosomes are circulating extracellular vesicles that carry genetic information for cell–cell communication and have recently attracted much attention because they carry DNA, RNA, and proteins.[2,3] Recent studies have reported experimental evidence, suggesting a relation between exosomes and genetic diseases, such as Parkinsonian tremor, Alzheimer's, diabetes mellitus, and several cancers.[1,4-6] These results also showed that exosomes hold promise as medical tools,[7-9] for example for drug-delivery systems.[10]

Various technologies have led to instruments that aid sample preparation and analysis, such as fluorescence-activated cell sorters, ultra-centrifugal systems, DNA sequencers and electron microscopes.[11,12] A technology for preparing high-quality and high-density exosome samples is important for their accurate analysis. High-density samples are often prepared using ultracentrifuges due to the compatibility of the technique for processing large samples, and the simple principle behind the technique and facile handling of the sample. However, there are growing concerns that a strong centrifugal force can damage samples, given that a centrifugal force of $100000 \times g$ or more must be applied to each sample for 1 – 2 h.[12] The use of filtration membranes without ultracentrifugation can result in damage, such as removal of the lipid membrane due to physical pressure and shear stress. Collection methods based on antibody–antigen reactions must consider the effects of the attached compound. Additionally, all of these methods are batch processes. There is therefore need for a rapid methodology for the isolation and concentration of exosome samples that do not cause damage.

The emerging technology of microfluidics[13-15] may help realize the versatile manipulation of small quantities of liquid sample by taking advantage of the scale effects of miniaturization.[16-18] Of the many approaches studied, the use of an electrical filtration device utilizing an ion-depletion zone in a microchannel may allow for the simultaneous continuous isolation and concentration of various volumes and types of liquid samples.[19-21] However, to date there has been no report describing either the interaction between the ion-depletion zone and exosomes or the effects of the induced physical and physiological changes on the characteristics of exosomes.

In this study, we experimentally observed the interaction between exosomes and the ion-depletion zone in a microfluidic device as an initial evaluation for exosome handling. We also used microscopic observation to quantitatively investigate the percent of damaged exosomes and morphological changes caused by the concentration process.

† To whom correspondence should be addressed.
E-mail: mogi.k@aist.go.jp (K. M.); ytakatoki@gmail.com (T. Y.)

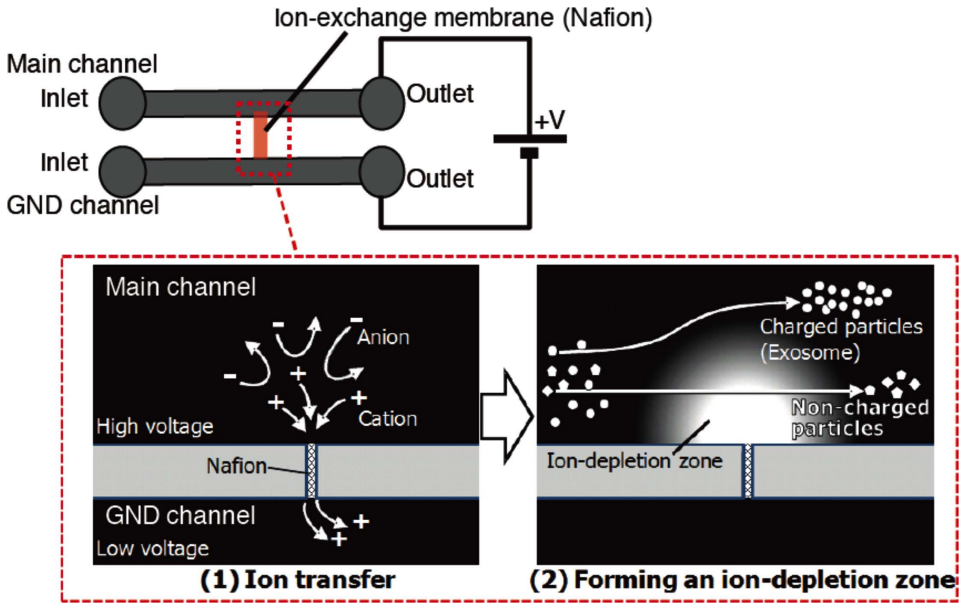

Fig. 1 Schematic showing the generation of an ion-depletion zone. An ion-depletion zone is formed by applying a voltage between two microchannels bridged by an ion-exchange membrane. (1) Cations that are drawn into and anions are pushed away from the edge of the Nafion membrane on the high-voltage side by an electrostatic force. (2) The generated ion-depletion zone is used as an intangible barrier against the entry of charged particles. A Nafion pattern intersects the Main and the GND channels. The inlet and outlet ports of the channels are in contact with the electrodes to apply an electric potential difference between the two microchannels.

Experimental

Ion-depletion zone for handling exosomes

An ion-depletion zone[19] is an area, from which all positively and negatively charged particles are excluded. Figure 1 shows a schematic of the generation of an ion-depletion zone in a microchannel. Two microchannels, designated as the Main channel and the GND channel, are bridged by a cation-exchange membrane (Nafion, 274704-25ML, Sigma-Aldrich). The application of a voltage between the two microchannels causes cations around the bridged area of the high-voltage side (in the Main channel) to be drawn into the low-voltage side of the GND channel through the Nafion membrane, as shown in Fig. 1(1). This increases the number of anions compared to cations, resulting in an instantaneous expulsion of anions by electrostatic repulsion and re-establishment of an electroneutral condition. This generates an ion-depletion zone, as shown in Fig. 1(2). No charged particles can enter this zone if the electrostatic force required to generate the ion-depletion zone is greater than the driving force required to move particles into the zone. In other words, the ion-depletion zone works as an intangible barrier against any charged particle. Since exosomes are usually negatively charged, they are likely to be pushed to the other side of the microchannel under the force of a pressure-driven flow through the ion-depletion zone, as shown in Fig. 1(2).

Exosome preparation

Four types of exosomes were obtained: from a human umbilical vein endothelial cell line (HUVEC, C2517A, Lonza), a human cell line derived from breast adenocarcinoma (MCF-7, RCB1904, Riken Bioresource Center), a human embryonic kidney cell line (HEK293, RCB1637, Riken Bioresource Center), and a lung carcinoma cell line (A549, RCB0098, Riken Bioresource Center). Cells were seeded at 5.0×10^3 cells/cm^2 in 100 mm in diameter dishes (3020-100-MYP, IWAKI Co., Ltd.) and incubated at 37°C in an incubator with 5% CO_2. The medium was replaced every three days. The cells reached confluence after two weeks and exosomes were collected from the culture medium using a filter kit (exoEasy Maxi Kit, Qiagen). The exosomes, of unknown concentration, were stained with PKH26 (PKH26 Red Fluorescent Cell Linker Kit, Sigma-Aldrich).

Device fabrication

The device contained two identical areas for evaluating the ion-depletion zone. The device was composed of microchannels, named as the Main and GND channel, made of polydimethylsiloxane (PDMS),[13] a glass substrate with electrodes, and a Nafion pattern on top, as shown in Fig. 1. The size of the Main channel is 1 mm in width and 100 µm in depth, and that of the GND channel is 2 mm in width and 100 µm in depth. To generate an electric potential difference between the two channels, each port of the channel is aligned on the electrode patterns on the glass substrate. The fabrication process of the microfluidic device with the Nafion pattern is as follows (Fig. S1, Supporting Information). The electrode patterns, made of an Au layer 200 nm thick and a Cr layer 5 nm thick on a glass substrate, were fabricated by a conventional sputtering and wet-etching process. The Cr layer was used as an adhesive layer between the Au electrodes and the glass substrate (Fig. S1(a)). Next, Nafion was patterned on the glass substrate by a molding technique. The mold for the Nafion pattern was a channel structure 100 µm wide and 25 µm height fabricated by a molding PDMS substrate. A 0.6% Nafion solution in ethanol was injected into the mold (Fig. S1(b)). The mold containing the Nafion solution was heated for 10 min at 100°C (Fig. S1(c)), and then the mold was peeled from the glass substrate and the

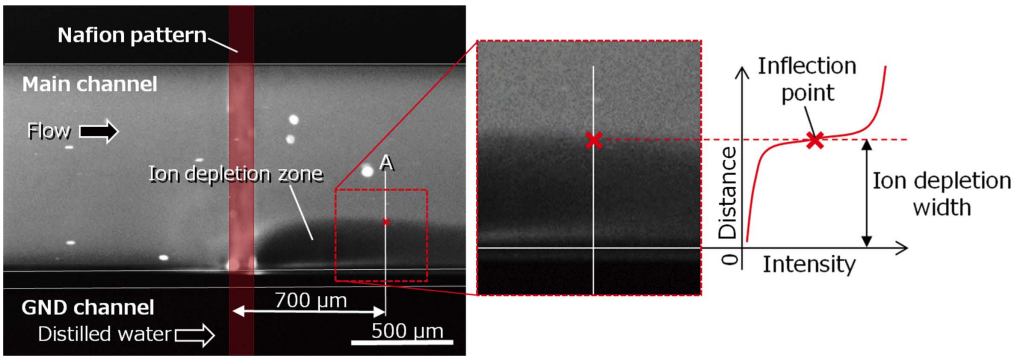

Fig. 2 Fluorescence image of exosomes in the Main channel near the Nafion pattern. Exosomes were supplied from the left to the right through the Nafion pattern and the generated ion-depletion zone. The distribution of the fluorescence intensity on line A was measured to quantify the extent of the ion-depletion zone. The inflection point on the intensity curve of the exosome stream on line A is defined as the boundary of the ion-depletion zone.

presence of the solidified subnanometer-thick Nafion pattern was confirmed on the glass substrate (Fig. S1(d)). Finally, a PDMS substrate comprising a Main channel and a GND channel was placed on the glass substrate with positioning the Nafion pattern to the channels (Figs. S1(e) and S1(f)).

Experimental setup

The relation between the applied voltage and the flow rate, and the size of the ion-depletion zone, was evaluated by observing the interaction between exosomes and the ion-depletion zone using the setup shown in Fig. S2 (Supporting Information). The outlet ports of the microchannels were connected with a syringe pump, and then set on a microscope stage (IX-73, Olympus Corp.). Events in the microchannel were observed by fluorescence imaging using a CCD camera (DP72, Olympus Corp.).

Evaluation of exosome handling in the ion-depletion zone

We evaluated the effect of the ion-depletion zone in the Main channel on exosomes by observing the fluorescent intensity of exosomes injected into the Main channel. The concentration of exosomes was estimated from the fluorescence intensity because it is generally difficult to determine the absolute amount of exosomes. The exosome concentration was estimated from the fluorescence intensity using the Lambert-Beer law. This value is given as

$$I = I_0 C\phi\varepsilon \exp(-\varepsilon x C). \quad (1)$$

Here, I is the intensity of the fluorescence, I_0 is the flux of the excitation light, C is the concentration of exosomes, ϕ is the fluorescence quantum yield, ε is the absorbance index and x is the light-path length.

The exponential part of the Eq. (1) can be removed due to the negligible value of x and the low concentration C in the microchannel experiment. Hence, the fluorescence intensity increases linearly with concentration at low exosome concentrations.

Evaluation of the number exosomes

The exosomes were confirmed to be dome-shaped and their density was quantified from images, as shown in Fig. S3 (Supporting Information). The densities of exosome were calculated from the average number of exosomes measured in a $200 \times 200\ \mu m^2$ area. The raw AFM images were flattened, binarized, threshold denoised, detected the boundary of particles, and finally counted the number using image processing software ImageJ.

Results and Discussion

Interaction between the ion-depletion zone and the exosomes

We observed the interaction between the ion-depletion zone and exosomes prepared from HUVEC. Figure 2 shows a fluorescence image of exosomes in the ion-depletion zone in the microchannel. The flow rate was 1 µL/min and the applied voltage was 100 V. The white-colored area corresponds to the dispersion of exosomes, visualized as a cloud of small exosome particles. The Nafion pattern used to generate the ion-depletion zone is located in the middle of the microchannel, as shown in the figure. The exosome solution flows from left to right, and thus the ion-depletion zone, shown as a black-colored area, is generated on the downstream side of the Nafion pattern. The width of the ion-depletion zone, measured to quantitatively evaluate the extent of the ion-depletion zone in this work, is defined as the width of the zone on line "A" in Fig. 2, which is located 700 µm from the edge of the Nafion pattern. In the inset of Fig. 2, the inflection point of the curve fit to the fluorescence intensity on line "A" was defined as the boundary of the ion-depletion zone. This image processing provided the width of the ion-depletion zone as the distance from the wall of the Main channel to the boundary of the stream.

Figure 3(a) shows the correlation between the width of the ion-depletion zone and the flow rate under an applied voltage of 100 V. The width of the ion-depletion zone decreased with increasing flow rate. The ion-depletion zone should essentially fill the microchannel if the widths of the microchannel and ion-depletion zones are identical; the latter can be controlled by the flow rate. Figure 3(b) shows the relation between the width of the ion-depletion zone and the driving voltage at a flow rate of 1 µL/min. This flow rate provides the maximum ion-depletion width in Fig. 3(a). The shape of the graph is approximately linear, the gradient is about 3.9 µm/V over the range 0 to 80 V, and then tends to saturate at 80 V or higher. These results indicate that the width of the ion-depletion zone in the stream of exosomes in the microchannel is controlled by both the flow rate and the driving voltage.

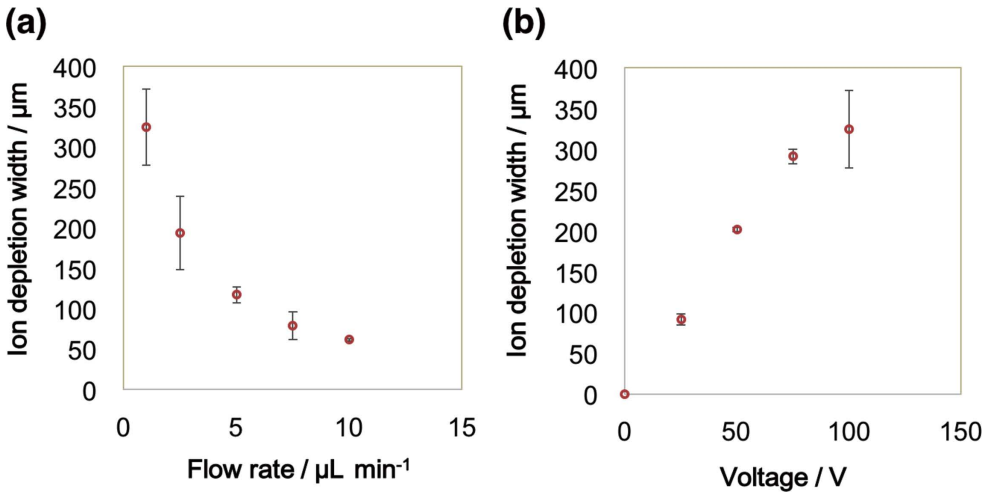

Fig. 3 Relation between the width of the ion-depletion zone and the flow rate (a), as well as the width of the ion-depletion zone and the driving voltage at a flow rate of 1 μL/min (b), respectively. Each value is the average of five trials, and the error bars are the standard deviation.

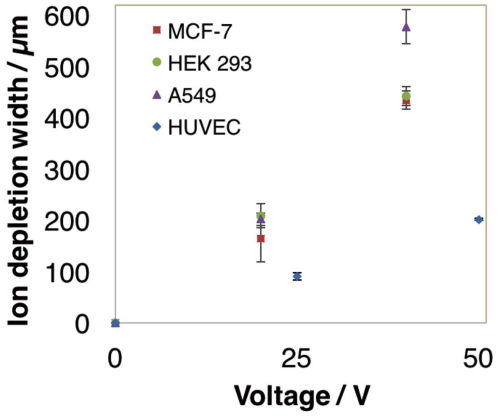

Fig. 4 Width of the ion-depletion zone depends on the driving voltage. Exosomes were obtained from the culture medium of MCF-7, HEK293, A549, and HUVEC cells. Each relation was obtained using 1 μL/min flow streams of the exosomes.

Extent of the ion-depletion zone depends on the type of exosome

We next investigated the extent of the ion-depletion zone with respect to the type of exosome. Figure 4 shows that the driving voltage depended on the width of the ion-depletion zone for 1 μL/min flow streams containing MCF-7, HEK 293, and A549 exosomes. The width of the ion-depletion zone for all exosome types shows nearly the same trend, except for exosomes from HUVEC. The mechanism behind the voltage responses remains unknown; however, the results clearly show that the width of the ion-depletion zone in the stream of exosomes is controlled well by the driving voltage, regardless of the type of exosome, indicating that exosomes from any source can be manipulated by controlling the ion-depletion zone.

Damage to the exosomes caused by the ion-depletion zone

The direct and the indirect damages, caused not only by the physical breaking down of exosome due to centrifugal force or electrical interactions, but also by the adhesion of exosomes onto the surface of centrifugal tube or microchannel, would lead a reduction in the density of exosomes, respectively. Therefore, the yield of exosomes passing through the ion-depletion zone was investigated to evaluate damage to the exosomes caused by the ion-depletion zone. For this purpose, we visualized the shapes and densities of the exosomes using an AFM,[9,22-24] as shown in Fig. 5. We prepared four samples, which were delivered from the same exosome solution. The first portion was directly used as a pretreatment sample (Fig. 5(a)); the second one was treated by an ultra-centrifugal process (Fig. 5(b)); the third one was treated by the ion-depletion zone with applied voltage at 30 V (Fig. 5(c)); and the forth one was treated with the ion-depletion zone with the applied voltage at 100 V (Fig. 5(d)). The exosomes after the ultra-centrifugation were mildly stirred and dispersed to the original volume of the medium. The exosomes after treatment with the ion-depletion zone in the device waere collected from the outlet of the microfluidic device during flowing the sample so as to avoid an enrichment of exosomes by evaporation. Those samples were dispersed on a glass slide, and visualized using an atomic-force microscope (Bruker Dimension Icon with ScanAsyst, BRUKER).

We assumed that the density of the exosomes would decrease if they were damaged. The level of damage following passage through the ion-depletion zone to that inflicted by standard ultra-centrifugal separation was compared. Possible damage resulting from the centrifugal force was applied by concentration and redispersion at a centrifugal force of 134000 × *g* for 70 min at 4°C by using an ultra-centrifugal system (Optima™ L-100 XP and SW41Ti, Beckman Coulter, Inc.).[25,26] Figure 5(e) shows the density of the exosomes, that is the number of exosome particles per measured area (200 μm × 200 μm). The density of exosomes after ultra-centrifugation was about 43% lower (7.3×10^5 particles/mm^2 compared to 16.9×10^5 particles/mm^2) compared with the pretreatment sample, whereas only a 2% decrease occurred, compared with the pretreatment sample that was observed following passage through the ion-depletion zone, as shown in the figure. This result clearly shows that the ion-depletion technique damages exosomes less than a centrifugal technique.

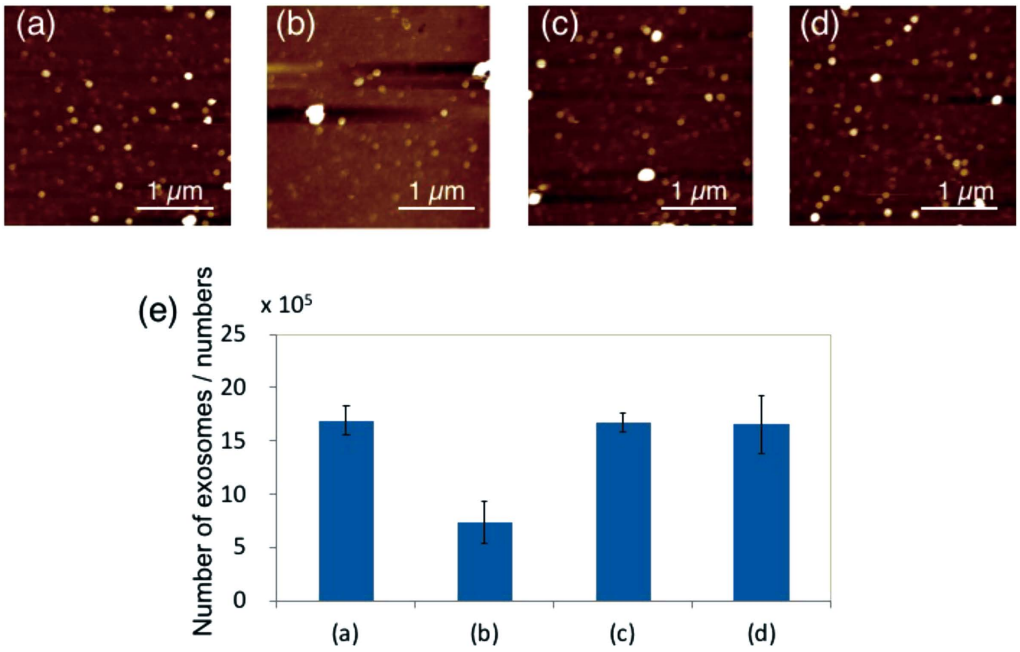

Fig. 5 AFM images of exosomes and the number of exosome particles following treatment under different conditions: (a) pretreatment sample, (b) ultra-centrifugal processed sample, and samples subjected to the ion-depletion zone using an applied voltage of (c) 30 V or (d) 100 V, respectively. Graph (e) shows the counted number of exosome particles per the measured area (200 μm × 200 μm). The exosomes were obtained from the culture medium of MCF-7 cells. Each value is the average of four results and the error bars indicate the standard deviation.

Conclusions

We proposed an electrical method using an ion-depletion zone for handling exosomes, which processes the exosome particles with low damage. As a proof-of-concept, we developed a prototype microfluidic device capable of generating an ion-depletion zone in a microchannel. We focused on evaluating the controllability of the exosomes using the effect of the ion-depletion zone by changing the flow rate of the exosome stream and the driving voltage to generate an ion-depletion zone. We demonstrated that the ion-depletion zone exerts a force on exosomes, regardless of their source. Exosomes in a flow stream were pushed from the ion-depletion zone, the size of which was controlled by the flow rate and the driving voltage of the ion-depletion zone. Damage to the exosomes caused by the ion-depletion zone was evaluated to investigate the yield of exosomes following passage through the ion-depletion zone. The extent of damage was compared with that caused by a conventional ultra-centrifugation method. Ultracentrifugation provided a yield of 57%, whereas a yield of 98% or more was obtained using the ion-depletion zone technique, thereby demonstrating that the ion-depletion-zone-based method causes less damage than the centrifugation method.

The use of the ion-depletion zone method for handing exosomes is in its infancy, yet ion-depletion has a potential for various applications, such as the concentration, and separation by taking advantage of type-specific changes in motion, thereby enhancing the study of exosomes.

Acknowledgements

JSPS KAKENHI Grant Numbers 17H03246, a Grant-in-Aid for Young Scientists (B) (Nos. 15K20989 and 17K17715), and JKA RING!RING! Project for the financial support (FY2015, No. 27-183).

Supporting Information

This material is available free of charge on the Web at http://www.jsac.or.jp/analsci/.

References

1. J. Skog, T. Wurdinger, S. van Rijn, D. H. Meijer, L. Gainche, M. Sena-Esteves, W. T. Curry, B. S. Carter, A. M. Krichevsky, and X. O. Breakefield, *Nat. Cell Biol.*, **2008**, *10*, 1470.
2. H. Valadi, K. Ekstrom, A. Bossios, M. Sjostrand, and J. Lotvall, *Allergy*, **2007**, *62*, 372.
3. H. Valadi, K. Ekstrom, A. Bossios, M. Sjostrand, J. J. Lee, and J. O. Lotvall, *Nat. Cell Biol.*, **2007**, *9*, 654.
4. M. J. Haney, N. L. Klyachko, Y. L. Zhaoa, R. Gupta, E. G. Plotnikova, Z. J. He, T. Patel, A. Piroyan, M. Sokolsky, A. V. Kabanov, and E. V. Batrakova, *J. Controled Release*, **2015**, *207*, 18.
5. L. Rajendran, M. Honsho, T. R. Zahn, P. Keller, K. D. Geiger, P. Verkade, and K. Simons, *Proc. Natl. Acad. Sci. U. S. A.*, **2006**, *103*, 11172.
6. S. Saman, W. Kim, M. Raya, Y. Visnick, S. Miro, S. Saman, B. Jackson, A. C. McKee, V. E. Alvarez, N. C. Y. Lee, and G. F. Hall, *J. Biol. Chem.*, **2012**, *287*, 3842.
7. L. Alvarez-Erviti, Y. Q. Seow, H. F. Yin, C. Betts, S. Lakhal, and M. J. A. Wood, *Nat. Biotechnol.*, **2011**, *29*, 341.
8. S. Ohno, M. Takanashi, K. Sudo, S. Ueda, A. Ishikawa,

N. Matsuyama, K. Fujita, T. Mizutani, T. Ohgi, T. Ochiya, N. Gotoh, and M. Kuroda, *Mol. Ther.*, **2013**, *21*, 185.
9. H. Kalra, C. G. Adda, M. Liem, C. S. Ang, A. Mechler, R. J. Simpson, M. D. Hulett, and S. Mathivanan, *Proteomics*, **2013**, *13*, 3354.
10. D. M. Sun, X. Y. Zhuang, X. Y. Xiang, Y. L. Liu, S. Y. Zhang, C. R. Liu, S. Barnes, W. Grizzle, D. Miller, and H. G. Zhang, *Mol. Ther.*, **2010**, *18*, 1606.
11. K. Carayon, K. Chaoui, E. Ronzier, I. Lazar, J. Bertrand-Michel, V. Roques, S. Balor, F. Terce, A. Lopez, L. Salome, and E. Joly, *J. Biol. Chem.*, **2011**, *286*, 34426.
12. C. Lasser, M. Eldh, and J. Lotvall, *J. Vis. Exp.*, **2012**, *59*, e3037.
13. K. Mogi and T. Fujii, *J. Micromech. Microeng.*, **2010**, *20*, 055015.
14. K. Aizel, Y. Fouillet, and C. Pudda, *J. Nanopart. Res.*, **2014**, *16*, 2731.
15. H. F. Arata, M. Kumemura, N. Sakaki, and H. Fujita, *Anal. Bioanal. Chem.*, **2008**, *391*, 2385.
16. H. Craighead, *Nature*, **2006**, *442*, 387.
17. M. I. Mohammed and M. P. Y. Desmulliez, *Lab Chip*, **2011**, *11*, 569.
18. K. Mogi, Y. Sugii, T. Fujii, and Y. Matsumoto, in Proceedings of the 11th International Conference on Nanochannels, Microchannels, and Minichannels, **2013**, Sapporo, Japan, ICNMM2013-73164.
19. S. J. Kim, S. H. Ko, K. H. Kang, and J. Han, *Nat. Nanotechnol.*, **2010**, *5*, 297.
20. S. J. Kim, Y. A. Song, and J. Han, *Chem. Soc. Rev.*, **2010**, *39*, 912.
21. K. Mogi, K. Hayashida, T. Yamamoto, *Electron. Commun. Jpn.*, **2017**, *100*, 56.
22. S. Sharma, H. I. Rasool, V. Palanisamy, C. Mathisen, M. Schmidt, D. T. Wong, and J. K. Gimzewski, *ACS Nano*, **2010**, *4*, 1921.
23. V. Palanisamy, S. Sharma, A. Deshpande, H. Zhou, J. Gimzewski, and D. T. Wong, *PLoS One*, **2010**, *5*, e8577.
24. N. Regev-Rudzki, D. W. Wilson, T. G. Carvalho, X. Sisquella, B. M. Coleman, M. Rug, D. Bursac, F. Angrisano, M. Gee, A. F. Hill, J. Baum, and A. F. Cowman, *Cell*, **2013**, *153*, 1120.
25. S. Flamant and R. Tamarat, *Radiat. Res.*, **2016**, *186*, 203.
26. M. L. Squadrito, C. Baer, F. Burdet, C. Maderna, G. D. Gilfillan, R. Lyle, M. Ibberson, and M. De Palma, *Cell Rep.*, **2014**, *8*, 1432.